Elemental carbon measurements in European Arctic snow packs

S. Forsström,[1] E. Isaksson,[1] R. B. Skeie,[2] J. Ström,[3] C. A. Pedersen,[1] S. R. Hudson,[1] T. K. Berntsen,[2,4] H. Lihavainen,[5] F. Godtliebsen,[1,6] and S. Gerland[1]

Received 21 March 2013; revised 26 November 2013; accepted 26 November 2013; published 26 December 2013.

[1] Black carbon (BC) and other light-absorbing particles deposited on snow and ice are known to perturb the surface radiative balance. There are few published observations of the concentration of these particles in the snow in Scandinavia and the European Arctic. We measured BC concentrations in snow samples collected in this region from 2007 to 2009, and we present the results here. The data set includes 484 surface samples and 24 column samples (covering the accumulation season) from snow on land, glaciers, and sea ice. Concentrations up to 88 ng of carbon per gram of snow (ng/g) were found in Scandinavia, while lower values were observed at higher latitudes: 11–14 ng/g in Svalbard, 7–42 ng/g in the Fram Strait, and 9 ng/g in Barrow. Values compare well with other observations but are generally found to be a factor of 2–3 higher than modeled BC concentrations in snow in the chemical transport model Oslo CTM2. This model underestimation comes in spite of potentially significant undercatch in the observations. The spring melt period enhanced BC levels in surface snow at the four sites where the BC concentrations were monitored from March to May in 2008 and 2009. A data set of replicate samples is used to establish a concentration-dependent estimate of the meter-scale variability of BC concentration in snow, found to be around ±30% of the average concentration.

Citation: Forsström, S., E. Isaksson, R. B. Skeie, J. Ström, C. A. Pedersen, S. R. Hudson, T. K. Berntsen, H. Lihavainen, F. Godtliebsen, and S. Gerland (2013), Elemental carbon measurements in European Arctic snow packs, *J. Geophys. Res. Atmos.*, *118*, 13,614–13,627, doi:10.1002/2013JD019886.

1. Introduction

[2] Black carbon (BC) particles are emitted to the atmosphere through incomplete burning and have both natural (grassland and forest fires) and anthropogenic (agricultural fires, domestic fire places, flaring, and combustion engines) sources [*Bond et al*., 2004; *Stohl et al*., 2013]. BC is a very efficient light absorber, impacting radiation budgets both as an atmospheric aerosol and as an impurity in snow and ice [*Bond et al*., 2013]. The additional absorption of sunlight caused by BC in the snowpack enhances snow grain growth and triggers an earlier spring melt [*Flanner et al*., 2007]. The effect of the earlier melt of ice and snow is enhanced by the positive albedo feedback, adding to the importance of the light-absorbing pollutants. Recently published observations are leading to an ever clearer picture of the ambient concentrations of BC in the snow in polar regions [*Doherty et al*., 2010; *Forsström et al*., 2009; *Hegg et al*., 2009, 2010] and at lower latitudes [*Ye et al*., 2012; *Huang et al*., 2010; *Wang et al*., 2013a; *Zhang et al*., 2013].

[3] The most comprehensive effort to map the concentration of light-absorbing particles in snow across the Arctic was made by *Clarke and Noone* [1985] and *Doherty et al*. [2010]. However, they present few data points for northern Scandinavia. The motivation of the present study is to improve the mapping for this area, which is of special interest since model estimates show that this region is the area with the highest BC concentrations in the Arctic [*Flanner et al*., 2007; *Koch et al*., 2009]. We present measurements of elemental carbon (EC) concentration in snow samples collected from 2007 to 2009. EC (elemental carbon) concentration is often used to represent BC (black carbon) concentration [*Andreae and Gelencsér*, 2006; *Bond et al*., 2013]. The quantities and terms EC and BC have been defined based on the analytical method used (see *Petzold et al*. [2013] for a full discussion of EC/BC terminology). Thermal or refractory methods result in EC measurements, while optically based absorption measurements result in BC concentrations. Our data set includes EC concentration from 263 surface

[1]Norwegian Polar Institute, Tromsø, Norway.
[2]Center for International Climate and Environmental Research-Oslo (CICERO), Oslo, Norway.
[3]Department of Applied Environmental Science, Stockholm University, Stockholm, Sweden.
[4]The Faculty of Mathematics and Natural Sciences, University of Oslo, Oslo, Norway.
[5]Finnish Meteorological Institute, Helsinki, Finland.
[6]The Faculty of Science and Technology, University of Tromsø, Tromsø, Norway.

Corresponding author: E. Isaksson, Norwegian Polar Institute, N-9005, Tromso 9296, Norway. (elisabeth.isaksson@npolar.no)

2169-897X/13/10.1002/2013JD019886

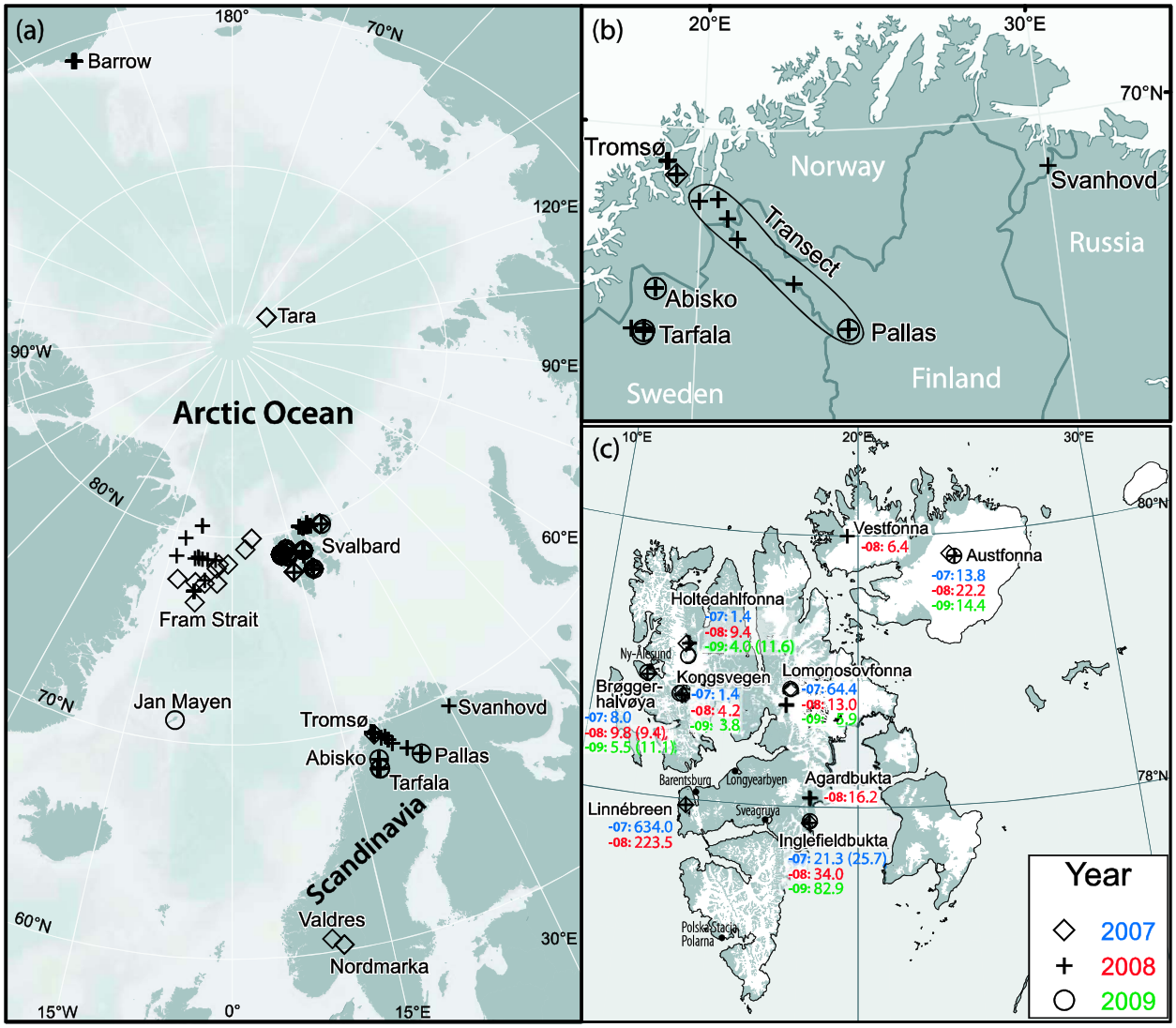

Figure 1. (a) Map of all sampling sites, (b) map of sampling sites in northern Scandinavia, and (c) map of sampling sites in Svalbard together with measured apparent elemental carbon concentrations in ng/g for March to April (all spring samples in parenthesis) 2007, 2008, and 2009. Values are medians at each site.

snow samples and 24 column profiles from Svalbard, Scandinavia, Barrow, and Arctic sea ice. At many of the 263 surface sampling sites, multiple samples were collected from within 1 m of each other and processed separately, providing a total of 484 individual EC measurements in surface snow.

[4] Measuring particles in snow is relatively challenging because of their low concentrations and small size. Most measurement techniques involve first melting a snow sample and passing it through a filter to collect the particles. The thermal optical method used in this study and in *Forsström et al.* [2009] and *Aamaas et al.* [2011] is a filter-based method in which particulate carbon is volatilized in two steps by exposing the substrate to high temperatures, first in an environment without oxygen, then in an environment with oxygen. The first step removes carbonate and organic carbon (OC), and the second step burns off EC. The volatilized carbon released during the two heating stages is measured to separately determine the mass of EC and other carbon on the filter. Correction for charring (conversion of OC to EC on the filter) during the first heating stage was done using the transmission method [*Birch*, 2003]. Some studies [e.g., *Ming et al.*, 2008] have used similar thermal optical methods with additional preheating or acid soaking steps to remove carbonates. *Warren and Clarke* [1990], *Grenfell et al.* [2002], *Warren et al.* [2006], *Doherty et al.* [2010], and *Wang et al.* [2013a] used a filter-based optical method (ISSW: Integrating Sphere/Integrating Sandwich method) for determining concentrations of insoluble light-absorbing particulates (ILAP) by measuring light absorption by particles on the filter. They separate the ILAP concentrations into BC and other light-absorbing matter using standards for BC light absorption. An additional commonly used method that does not involve filtration is based on counting individual particles with a single-particle soot photometer [*Schwarz et al.*, 2008]. This method has been used by *McConnell et al.* [2007] and *Kaspari et al.* [2011] for the detection of BC in ice cores from the Greenland ice cap and from a Himalayan glacier, respectively.

[5] Amounts of light-absorbing particles detected by different methods can vary considerably [*Watson et al*., 2005; *Schwarz et al*., 2012]. In addition to differences between the analysis methods, large spatial variability in snow impurity concentrations has been observed [*Doherty et al*., 2010; *Aamaas et al*., 2011; *Svensson et al*., 2013]. This study contributes to the estimation of the representativeness of snow samples analyzed for pollutants by presenting a large data set of replicate samples collected within a meter of each other at the same time and from the same snow layer.

[6] A recent multimodel study [*Lee et al*., 2013] showed that models severely underestimate the observed enhanced Arctic winter and spring near-surface atmospheric BC concentration. The same study also found that the modeled BC concentration in snow was, on average, within a factor of 2 to 3 of the measurements, except for the Arctic Ocean, where the concentration was significantly underestimated by the models. The episodic nature of some important pollution sources and the seasonality of the snow cover, aerosol deposition, and transport patterns are among the challenges for modeling BC in the Arctic atmosphere and its deposition in snow [*Shindell et al*., 2008; *Koch et al*., 2009; *Skeie et al*., 2011]. In this study the Oslo Chemical Transport Model 2 (CTM2) [*Berntsen et al*., 2006; *Myhre et al*., 2009; *Rypdal et al*., 2009; *Skeie et al*., 2011] is used to simulate the atmospheric transport and deposition of BC for the years 2007 through 2009, and the model results are compared to the measurements of EC in snow. Since emission factors used in the inventories are based on thermo-optical methods, comparing model results and measurements of EC should not include any methodological bias [*Vignati et al*., 2010]. When discussing model results or black carbon in general, we use the abbreviation BC, as is commonly used in the modeling community. When discussing our measurements we use the abbreviation EC, with [EC] referring specifically to the mass concentration of elemental carbon in our measurements.

2. Methods

2.1. Sampling and Analyses

[7] Snow samples were collected when the opportunity arose during various sea ice or glaciological field campaigns in 2007, 2008, and 2009. An overview of the sampling is given in Figure 1 and Tables 1 to 3. Samples were collected in Scandinavia, the Arctic archipelago of Svalbard, and Barrow, Alaska. In Svalbard (Figure 1c) annual visits by the Norwegian Polar Institute to the field sites of Brøggerhalvøya, Kongsvegen, Holtedahlfonna, Lomonosovfonna, and Austfonna were used for sampling, in addition to opportunistic sampling in Agardbukta, Inglefieldbukta, and Vestfonna. In addition samples were obtained from snow-covered sea ice during research cruises in Fram Strait, from Jan Mayen, and from the drifting station Tara.

[8] Weekly monitoring of surface snow [EC] was conducted throughout the spring at four sites: Austre Brøggerbreen, a glacier next to the atmospheric monitoring station Zeppelin on Brøggerhalvøya in Svalbard (2008, 2009); the atmospheric monitoring station in Pallas in northern Finland (2008 and 2009); Abisko research station in northern Sweden (2008 and 2009); and the meteorological office in Tromsø in northern Norway (2008). At the three latter sites the snow depth was also measured throughout the sampling seasons. In February 2008 a transect in northern Scandinavia was sampled (S18–S23 in Table 1), ranging in elevation from sea level at the Norwegian coast to an elevation of 560 m above sea level (asl) in northern Finland. In addition, individual samples were collected at the Norwegian sites of Svanhovd, Valdres, Nordmarka, and Tromsø.

[9] To investigate the column load (mg/m^2) of EC, samples were collected in vertical profiles through the snow pack, down to the ground, or down to previous summer surface on glaciers. EC column load was calculated using snow density measured at the time of sampling with a standard glaciological field method using a metal tube 20 cm in length to collect and weigh a known volume of snow. The column load was derived from [EC] measured in samples from layers between 2 and 20 cm in a vertical profile from top to bottom. The resulting vertical profile of EC mass was integrated to derive the column load.

[10] The surface samples were collected from the top 5 cm of snow, using small plastic shovels (4% of samples were from a different surface layer thickness, between 2 and 25 cm). Samples were collected in plastic bags or in glass jars. Snow was kept frozen until just before the filtering. Particles were collected on preheated quartz fiber filters (Munktel, 5.5 cm diameter) using electric or hand vacuum pumps and one of the following filtration setups:

[11] 1. The 2007 samples were melted at room temperature and filtered using a plastic funnel, cross-patterned filter holder, and small electrical pump. The part of the filter used for the analysis was taken in one of the quarters of the filter not influenced by the cross pattern on the filter holder.

[12] 2. An improved setup was used for samples collected in 2008 and 2009. The snow sample was placed into a glass funnel located inside a microwave oven that was then used for melting. Once the snow was melted, the whole sample was filtered through a filter sitting on a glass holder attached to the funnel under the microwave. The filter holder is made of sintered glass and yields a more even deposition of particles on the filter. The piece of the filter for analysis was taken from the middle of the filter.

[13] The filters were analyzed for elemental carbon using a thermal optical method (Sunset Laboratory Inc., Forest Grove, U.S., [*Birch and Cary*, 1996]) at Department of Applied Environmental Science, Stockholm University. The National Institute of Occupational Safety and Health (NIOSH)-5040 thermal sequence [*Birch*, 2003] was used to separate EC and other (carbonate and organic) carbon from the filter. The latest recommended temperature protocol European Supersites for Atmospheric Aerosol Research (EUSAAR2) [*Cavalli et al*., 2010] gives, on average, twice as large EC masses as NIOSH-5040, due to improved separation between the different types of carbon. In this paper the amounts of elemental carbon on each filter obtained using NIOSH-5040 are therefore multiplied by 2. The average EC mass on laboratory blanks, 29.5 ng/cm^2, was subtracted from all analyzed EC masses. For typical samples used in this study, this value corresponds to less than 6% of the observed EC mass.

2.2. The Oslo Chemical Transport Model

[14] The Oslo CTM2 model is an off-line chemical transport model driven with meteorological input data, run in this

Table 1. Median Elemental Carbon Concentrations ([EC]), With (25th and 75th Percentiles in Parentheses) for Each Site[a]

ID	Site	Date	[EC] (25–75% Percentile) (ng/g)	Sites	Subsites (Samples)	Description	Latitude	Longitude	Altitude (m asl)	h_{SWE}[b] (mm)	Comment[c]
S1	Fram Strait	21–27 Apr 2007	42.1 (13.3–88.2)	1	5 (5)	Sea ice	77.48	−7.34	0	93 [b]A	
S2	Fram Strait	15–26 Sep 2007	8.2 (0.0–18.7)	1	5 (5)	Sea ice	78.98	0.15	0	30 [b]A	
S3	Fram Strait	26 Apr to 27 May 2008	11.4 (5.6–15.7)	1	8 (14)	Sea ice	78.62	−7.57	0	108 [b]A	
S4	Fram Strait	02–08 Sep 2008	6.8 (3.8–7.4)	1	3 (4)	Sea ice	79.41	−9.97	0	15 [b]A	
S5	Tara	25 Apr 2007	12.3	1	1 (2)	Sea ice	87.92	130.05	0	112 [b]A	
S6	Barrow	14–19 Apr 2008	8.7 (5.9–11.4)	1	12 (34)	Sea ice, tundra	71.33	−156.43	0	58	
S7	Svalbard	25 Feb to 22 Apr 2007	13.8 (8.1–33.9)	**6**	13 (45)	Glacier, tundra, sea ice	78.76	16.00	622	401	
S8	Svalbard	11 Mar to 14 May 2008	13.0 (8.7–25.2)	**8**	43 (98)	Glacier, tundra, sea ice	78.81	17.21	482	588	
S9	Svalbard	27 Mar to 24 May 2009	11.4 (5.9–14.4)	**6**	33 (69)	Glacier, tundra, sea ice	78.88	16.39	600	450	
S10	Pallas	18 Jan to 23 May 2008	45.6 (30.5–89.4)	1	17 (21)	Treeline	67.97	24.12	510	335	
S11	Pallas	06 Mar to 05 May 2009	78.4 (50.5–150.9)	1	11 (11)	Treeline	67.97	24.12	510	312	
S12	Tarfala	12–14 Jul 2008	42.9 (42.5–60.5)	1	3 (9)	Tundra, glacier	67.93	18.47	1613	305	P
S13	Tarfala	05 Dec 2008 to 16 Apr 2009	14.5 (4.0–32.5)	1	6 (15)	Tundra	67.91	18.58	1300	-	P
S14	Abisko	24 Jan to 24 Apr 2008	51.4 (27.6–90.7)	1	15 (19)	Forrest	68.35	18.82	360	58 [b]B	
S15	Abisko	19 Nov 2008 to 23 Apr 2009	32.2 (17.5–41.8)	1	16 (16)	Forrest	68.35	18.82	360	64 [b]B	
S16	Tromsø	10 Jan to 20 May 2008	53.3 (31.3–95.1)	1	24 (86)	Town	69.65	18.94	94	178	P
S17	Jan Mayen	31 Mar 2009	21.3	1	1 (1)	Glacier	71.01	−8.20	1000	684	
S18	Tran6	20 Feb 2008	16.8	1	1 (3)	Forrest, field	69.26	19.92	8	382 [b]C	M
S19	Tran5	20 Feb 2008	13.7	1	1 (3)	Forrest	69.29	20.46	150	188 [b]B	M
S20	Tran4	20 Feb 2008	10.6	1	1 (3)	Tundra	69.09	20.76	548	263 [b]B	M
S21	Tran3	20 Feb 2008	19.9	1	1 (3)	Tundra	68.89	21.05	471	61 [b]D	M
S22	Tran2	20 Feb 2008	15.8	1	1 (3)	Forrest	68.44	22.64	320	44 [b]D	M
S23	Tran1	20 Feb 2008	32.5	1	1 (3)	Forrest	67.97	24.12	560	69 [b]D	M
S24	Svanhovd	14 Feb 2008	63.6	1	1 (1)	Forrest	69.47	30.05	30	114 [b]E	M
S25	Valdres and Nordmarka	19–20 Feb 2007	87.6 (44.5–130.6)	1	2 (7)	Forrest	60.42	10.05	760	81	P
S26	Tromsø Ramfjorden	06 Mar 2007	5.4	1	1 (1)	Sea ice	69.52	19.23	0	99 [b]E	M

[a]An average of measured or estimated snow water equivalent (h_{SWE}) in millimeters, together with the average of latitude, longitude, and altitude as meters above sea level, are included.

[b]For h_{SWE}, snow density ρ_s or/and snow depth h_s was not measured at site but estimated from the following: A, ρ_s from *Forsström et al.* [2011]; B, ρ_s from *Rasmus* [2005] and h_s from Norwegian Water Resources and Energy Directorate; C, ρ_s from same type of snow pack (C2) and h_s from Norwegian Water Resources and Energy Directorate; D, ρ_s from *Rasmus* [2005] and h_s from Finnish Meteorological Institute; E, ρ_s from same type of snow pack (C2).

[c]P, pollution from local sources; M, pollution from local sources might have occurred.

Table 2. Svalbard [EC] (Median Concentration Together With 25th and 75th Percentiles) in Surface Snow Samples at Different Sites[a]

ID	Site	Date	[EC] (kng/g)	Subsites (Samples)	Description	Latitude	Longitude	Altitude (m asl)	h_{SWE}[b] (mm)	Comment[c]
A1	Brøggerhalvøya	25 Mar to 01 Apr 2007	8.0 (7.1–9.1)	4 (15)	Glacier, tundra	78.88	11.98	158	197	
A2	Brøggerhalvøya	08 Jan to 27 May 2008	9.8 (6.0–17.1)	19 (23)	Glacier, tundra, sea ice	78.88	11.94	415	727	
A3	Brøggerhalvøya	20 Feb to 18Jun 2009	11.1 (4.7–32.7)	26 (55)	Glacier, tundra	78.87	11.92	273	431	
A4	Linnébreen	10 Apr 2007	634.0	1 (3)	Glacier	77.96	13.91	350	657	P
A5	Linnébreen	15 Apr 2008	223.5	1 (2)	Glacier	77.96	13.90	340	979	P
A6	Vestfonna	28 Apr 2008	6.4 (5.4–9.8)	10 (30)	Glacier	80.00	19.54	323	553	
A7	Austfonna	18 Apr 2007	13.8	1 (4)	Glacier	79.85	23.80	749	659	
A8	Austfonna	23 Apr 2008	22.2	1 (3)	Glacier	79.83	24.02	750	766	
A9	Austfonna	30 Apr 2009	14.4	1 (1)	Glacier	79.83	24.00	600	426	
A10	Lomonosovfonna	27 Mar 2007	64.4 (9.5–119.3)	2 (8)	Glacier	78.86	17.43	1250	430	
A11	Lomonosovfonna	07–09 Apr 2008	13.0 (7.3–20.5)	6 (18)	Glacier	78.75	17.28	709	721	
A12	Lomonosovfonna	27 Mar 2009	5.9 (5.3–6.5)	1 (2)	Glacier	78.86	17.43	1250	334	
A13	Holtedahlfonna	17 Apr 2007	1.4	1 (3)	Glacier	79.14	13.27	1124	286	
A14	Holtedahlfonna	30 Apr 2008	9.4	1 (4)	Glacier	79.14	13.39	1250	800	
A15	Holtedahlfonna	27 Apr 2009	11.6 ()	2 (8)	Glacier	79.14	13.39	1124	629	
A16	Kongsvegen	22 Apr 2007	1.4	1 (3)	Glacier	78.76	13.34	640	699	
A17	Kongsvegen	24 Apr 2008	4.2	1 (3)	Glacier	78.76	17.43	640	956	
A18	Kongsvegen	23 Apr 2009	3.8 (2.9–4.8)	2 (2)	Glacier	78.77	13.25	604	820	
A19	Inglefieldbukta	25 Feb to 25 Mar 2007	25.7 (19.1–36.3)	4 (12)	Tundra, sea ice	77.88	18.29	36	69 [b]A	M
A20	Inglefieldbukta	11–12 Mar 2008	34.0 (23.0–38.9)	4 (12)	Tundra, sea ice	77.88	18.29	36	57	M
A21	Inglefieldbukta	16 Apr 2009	82.9	1 (1)	Sea ice	77.90	18.31	0	56	M
A22	Agardbukta	13 Mar 2008	16.2	1 (5)	Tundra	78.07	18.27	5	127 [b]A	

[a]These samples, except Linnébreen, are used to calculate concentrations for Svalbard in Table 1. An average of measured or estimated snow water equivalent (h_{SWE}) in millimeters, together with the average of latitude, longitude, and altitude for eventual subsites, are given.
[b]For h_{SWE}, snow density was not measured at site but estimated from A, same type of snow pack C24.
[c]P, pollution from local sources; M, pollution from local sources might have occurred.

Table 3. Column Samples Analyzed for Elemental Carbon[a]

ID	Area	Site	Date	EC Column Load (mg m^{-2})	h_{SWE} (mm)	Description	Latitude	Longitude	Altitude (m asl)	Comment[b]
C1	Scandinavia	Nordmarka	19 Feb 2007	4.3	58	Forest	60.59	09.53	495	P
C2		Tromsø	07 Mar 2008	5.1	240	Town	69.65	18.93	100	P
C3		Tarfala Storglaciären	16 Apr 2009	14.6	1610	Glacier	67.92	18.58	1240	
C4	Svalbard	Corbel W	25 Mar 2007	3.0	153	Tundra	78.90		10	
C5		Nedre Brøggerbreen	01 Apr 2007	1.5	225	Tundra	78.91	11.83	20	
C6		Linnébreen	10 Apr 2007	171.2	657	Glacier	77.96	13.90	350	P
C7		Linnébreen	15 Apr 2008	165.0	979	Glacier	77.96	13.90	340	P
C8		Vestfonna BC 6	28 Apr 2008	6.6	486	Glacier	79.93	19.19	340	
C9		Vestfonna BC 7	30 Apr 2008	2.4	210	Glacier	79.94	19.13	195	
C10		Vestfonna BC 9	05 May 2008	12.2	798	Glacier	79.94	21.28	613	
C11		Austfonna Base 07	18 Apr 2007	4.2	659	Glacier	79.85	23.80	749	
C12		Austfonna Base 04	23 Apr 2008	12.7	766	Glacier	79.83	24.02	750	
C13		Austfonna Base 04	30 Apr 2009	9.3	426	Glacier	79.83	24.00	750	
C14		Lomonosovfonna summit	27 Mar 2007	10.2	431	Glacier	78.86	17.43	1250	
C15		Lomonosovfonna BC1	07 Apr 2008	4.2	328	Glacier	78.63	17.12	200	
C16		Lomonosovfonna BC2	07 Apr 2008	5.6	269	Glacier	78.72	17.28	400	
C17		Lomonosovfonna BC4	09 Apr 2008	8.6	668	Glacier	78.74	17.36	600	
C18		Lomonosovfonna summit	09 Apr 2008	16.8	1089	Glacier	78.86	17.43	1255	
C19		Lomonosovfonna summit	29 Mar 2009	4.3	334	Glacier	78.86	17.43	1250	
C20		Holtedahlfonna	30 Apr 2008	3.7	796	Glacier	79.14	13.39	1124	
C21		Kongsvegen Stake 8	22 Apr 2007	1.8	876	Glacier	78.76	13.34	640	
C22		Kongsvegen Stake 8	24 Apr 2008	5.2	983	Glacier	78.76	13.34	640	
C23		Kongsvegen Stake 6	23 Apr 2009	4.0	572	Glacier	78.78	13.15	534	
C24		Inglefieldbukta	16 Apr 2009	3.0	56	Sea ice	77.90	18.31	0	

[a]Sample ID, sampling site, date, EC column load (mg m^{-2}), measured snow water equivalent (h_{SWE}) in mm for the sampled snow column, latitude, longitude, and altitude in meters above sea level are shown.
[b]P, pollution from local sources.

study at horizontal resolution T42 ($2.8 \times 2.8°$). The model has been updated from the model used in *Skeie et al.* [2011]. The main differences are that large-scale precipitation is now removed every hour, rather than every third hour in the previous version, a bug was fixed in the snow module, and meteorological data are generated from cycle 36, rather than cycle 29, of the Integrated Forecast System model at the European Centre for Medium-Range Weather Forecasts. The emissions used in this study are the 2010 fossil fuel and biofuel emissions from the Representative Concentration Pathway (RCP) 8.5 is a so-called 'baseline' scenario that does not include any specific climate mitigation target. The greenhouse gas emissions and concentrations in this scenario increase considerably over time, leading to a radiative forcing of 8.5 W/m^2 at the end of the century [*Riahi et al.*, 2011] and monthly biomass burning emissions from the Global Fire Emissions Database version 3 [*Van der Werf et al.*, 2010]. The model was run, starting in August, for the years 2006–2007, 2007–2008, and 2008–2009. Meteorological input data and biomass burning emissions are specific for each year.

3. Results

3.1. Variability in the Snow Samples

[15] To investigate the meter-scale variability of [EC] in snow, 101 sets of replicate samples were collected during the surface snow sampling. For each set, two to five (most often three) samples were collected within 1 m of each other, at the same depth. The variability within a set was found to increase with concentration. A least squares fit indicates the standard deviation σ increases as

$$\sigma = 0.377\left[\overline{\mathrm{EC}}\right], \tag{1}$$

where the overbar indicates an average over all replicates in the set. Similarly, fits for the 25th and 75th percentiles as a function of median EC concentration ($[EC]_m$) were obtained:

$$[\mathrm{EC}]_{25\%} = 0.707[\mathrm{EC}]_m \tag{2}$$

$$[\mathrm{EC}]_{75\%} = 1.206[\mathrm{EC}]_m. \tag{3}$$

[16] Based on equations (1), (2), and (3), the meter-scale variability in the snow pack is on the order of ±30% of the average concentration. In addition to this meter-scale variability, the variability caused by the analysis method, discussed in section 5.4, is included in σ, $[EC]_{25\%}$, and $[EC]_{75\%}$. *Svensson* [2011] investigated repeated analyses of EC mass from individual filters, with the same thermal optical method used here. Based on his results, we estimate that the analytical variability in [EC] in our study accounts for less than 20% of the total standard deviation among [EC] values from replicate sampling, with most of the variability represented in equation (1) coming from real meter-scale variability within the snow, though sampling and filtering variations also contribute.

[17] Figure 2 shows the variability observed between the replicate samples. While the ratio of [EC] determined from replicate samples ($[EC]_1/[EC]_2$, where the subscript indicates sample number, chosen such that $[EC]_1 > [EC]_2$) is between

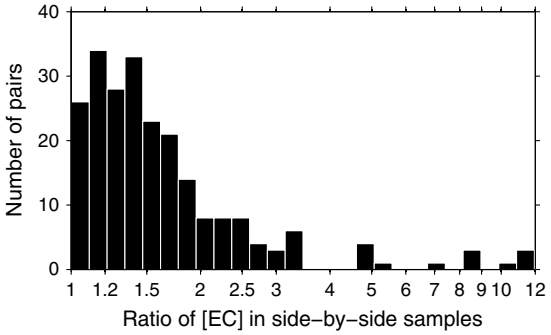

Figure 2. Variability in [EC] measured in replicate samples collected within a 1 m horizontal distance. At each site, two to five (usually three) replicates were collected. The histogram shows the ratio s_1/s_2 , where $s_1 > s_2$, for all replicate pairs (for sites with more than two replicates, all possible combinations are included).

1 and 1.4 for 47% of replicate pairs, 25% of pairs have a ratio between 1.5 and 2, and 5% have a ratio greater than 4. These large ratios illustrate the potential for large variability over small distances and suggest that sampling for BC concentration in snow should include several samples from each site to get a representative value.

3.2. EC Distribution in Surface Snow 2007–2009

[18] The distribution of [EC] in surface samples is close to lognormal (Figure 3), with a median [EC] (25th–75th percentile) for the whole data set of 16.3 (11.4–46.9) ng/g. Concentrations measured in different sampling areas and seasons are presented in Table 1. Table 2 shows detailed results from the Svalbard sampling sites. Most of the sites were out of range of any local pollution sources; sites which we know have local pollution sources are indicated with "P." Similarly, sites where local pollution might have occurred are marked with "M" in the tables. Where relevant, values reported here are medians over subsites and/or replicates.

[19] We found no link between snow water equivalent (h_{SWE}) and surface [EC], but h_{SWE} is included in Tables 1 and Table 2 as a measure of the snow accumulation at each site up to the time of the sampling. When snow depth (h_s) and density (ρ_s) were not measured during sampling (indicated by superscripted "b" in the tables), h_{SWE} was estimated using nearby measurements or values from the literature, as described in the footnotes to the tables.

[20] The site-median surface [EC] in Scandinavia varied between 5 and 88 ng/g and was generally higher than at the Arctic sampling locations (S1–S9 in Table 1). The highest concentrations within Scandinavia were measured near Oslo (S25) and close to the Russian border in Svanhovd (S24). Surface samples from Tromsø, a high-precipitation urban site, had a median [EC] of 53 ng/g, similar to remote but drier areas inland (Abisko, Pallas, and Tarfala, S10 through S15).

[21] Samples from Barrow and the drifting station Tara had lower concentrations than most of the Scandinavian mainland samples, with medians of 9 and 12 ng/g, respectively. Svalbard samples had intermediate median concentrations of 12–17 ng/g. The snow on drifting sea ice in the Fram Strait had low median concentrations (6.8 to 11.4 ng/g), except in spring 2007 when the median of five samples was 42 ng/g. A statistical test comparing Scandinavian with those from Svalbard and the Fram Strait (combined) confirms that the Scandinavian samples had significantly higher [EC]. The test holds for the whole data set, for springtime data only, and for individual years.

[22] Large variability between different sites and areas is expected since significant variability is found in side-by-side samples (section 4.1). Figure 1c shows the distribution of [EC] (as site medians) in surface snow in Svalbard, an area with systematic spring sampling. Despite the large variability, there does seem to be a pattern, with surface [EC] higher in the eastern part of Svalbard than in the western part in all years (ignoring locally polluted Linnébreen). The strongest gradient is seen in data from 2007, which were discussed by *Forsström et al*. [2009].

[23] The evolution of snow surface [EC] at four monitoring sites through spring 2008 and 2009 is presented in Figure 4, together with measured snow depths for three of the sites. At all sites, surface snow [EC] reached its maximum values in the months of March to May. The four monitoring sites have different pollution and precipitation levels, which are reflected in the measured concentrations. Brøggerhalvøya, a remote Arctic site, had low concentrations, ranging from 2.5 to 48.5 ng/g, with medians during the observation period of 9.8 in 2008 and 11.1 ng/g in 2009. Pallas and Abisko are remote subarctic sites with low precipitation rates (300 mm yr^{-1}). The median [EC] measured in the surface snow in Pallas during the observation period was 45.6 ng/g in 2008 and 78.4 ng/g in 2009. At Abisko, median observed values were 51.4 ng/g in 2008 and 32.2 ng/g in the 2008–2009 snow season. The urban sampling site in Tromsø receives large amounts of BC from the surrounding town, but the high precipitation rate (>1000 mm yr^{-1}) resulted in samples with a median [EC] of 53.3 ng/g, comparable to that in Abisko or Pallas. In Abisko and Brøggerhalvøya [EC] was generally higher in spring 2008 compared to spring 2009.

[24] The sampling site at Brøggerhalvøya is located on a glacier (440 m asl), with no monitoring of the snow depth during the sampling seasons. In both years, measurements

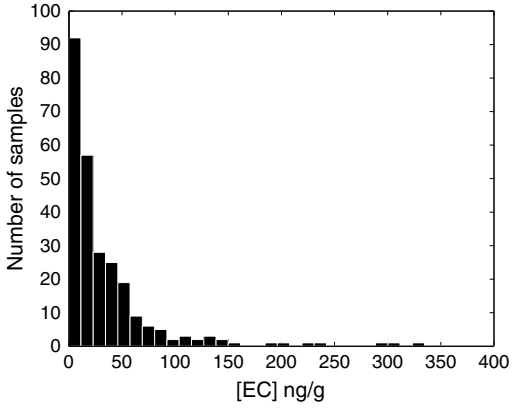

Figure 3. Histogram of all elemental carbon concentrations [EC], averaged over replicate samples and excluding two outliers from a site near a significant pollution source.

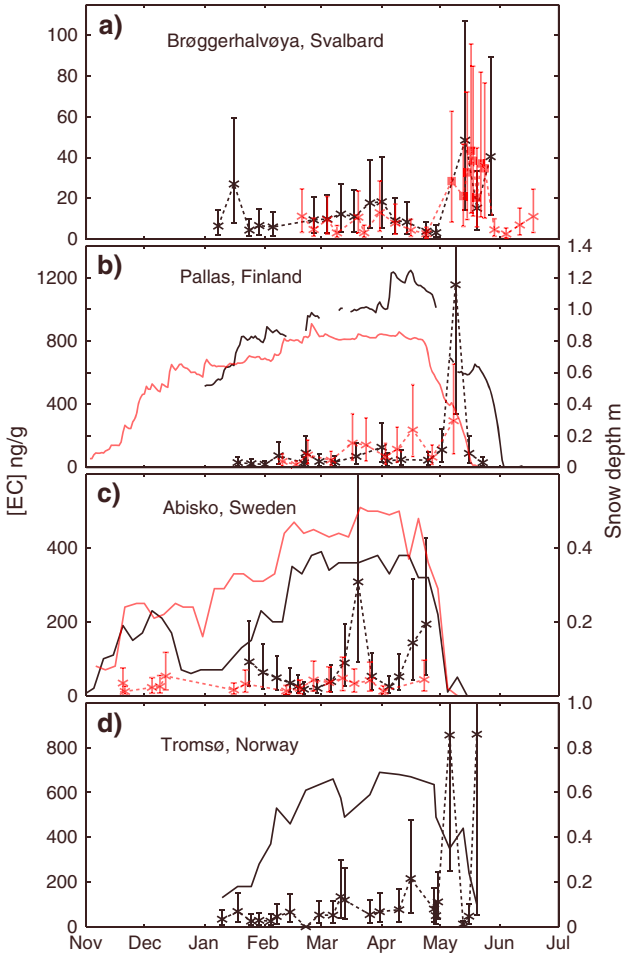

Figure 4. Elemental carbon concentration [EC] measured in the surface snow (top 5 cm) at four different monitoring stations over the snow seasons 2007–2008 (black) and 2008–2009 (red). The cross shows median values for replicate samples, and the error bars show the 25th and 75th percentiles, estimated with equations (2) and (3). (a) The Brøggerhalvøya sampling site is located on a glacier (440 m asl) near the atmospheric monitoring station Zeppelin. The square markers in May 2009 show samples collected close to the same glacier but at a lower elevation site (60 m asl). (b) Samples collected near the Pallas atmospheric monitoring station (510 m asl), from a site close to the tree line and therefore somewhat sheltered from winds. (c) Samples from Abisko are collected in a wind-protected site in a birch forest close to the Abisko research station. Brøggerhalvøya, Pallas, and Abisko can be considered remote sites, with minimal local pollution. (d) Samples collected in an urban site near downtown Tromsø, at the instrument field of the Norwegian Meteorological Institute (100 m asl). At the three latter sites snow depth (plotted as black (2008) and red (2009) solid lines) was monitored throughout the sampling period, in Pallas using automatic acoustic sensor and in Abisko and Tromsø by manual measurements.

in May have about 3 times higher concentrations than in the other months. Note that most of the May samples from 2009 were collected at a lower elevation site (60 m asl), somewhat closer to the settlement of Ny-Ålesund.

[25] The onset of snowmelt (as inferred from the snow depth data) occurred in Pallas during the last weeks of April. The highest measured surface EC concentrations followed a steep decrease in snow depth in both 2008 and 2009. The 2008 samples from Abisko show an order of magnitude increase in surface [EC] during April, but in 2009 there was no significant increase. In both years sampling was terminated around 10 days before the ground became snow free. In 2008, the snow pack in Tromsø started to decrease rapidly during the last days of April, leading to [EC] above 800 ng/g; lower values returned after a snow event in mid-May, and then another peak in concentrations came as melting resumed.

3.3. Model Comparison to Observations

[26] Column samples (Table 3) had column loads of EC ranging from 1.5 to 16.8 mg/m^2. The highest column loads were found at the glaciated sites Lomonosovfonna (in Svalbard) and Storglaciären (in Tarfala, Sweden). Linnébreen (in Svalbard, C6 and C7) is affected by strong local pollution (column load over 169 mg/m^2) and is thus not considered. Figure 5 compares the modeled BC column loads with the measured EC column loads, providing a comparison of the modeled and observed deposition over the whole snow season. The model underestimates the column load by up to a factor of 10. The sample in Nordmarka (in southern Norway) is an exception, where the model slightly overestimates the column load.

[27] Figure 6 shows the average concentration of modeled BC in surface snow (uppermost 5 cm) for the spring period in 2008. The medians of the observed [EC] values for the spring period (March–May) are also shown. The model captures the observed features with higher concentrations in Scandinavia than in the Arctic. Visual comparison shows good agreement in the Arctic and larger than observed values in northern Scandinavia in spring. In Figure 7 the measured surface concentrations are plotted against the modeled surface values for the corresponding day. In winter, the model underestimates the surface concentration by a factor of 3 in both

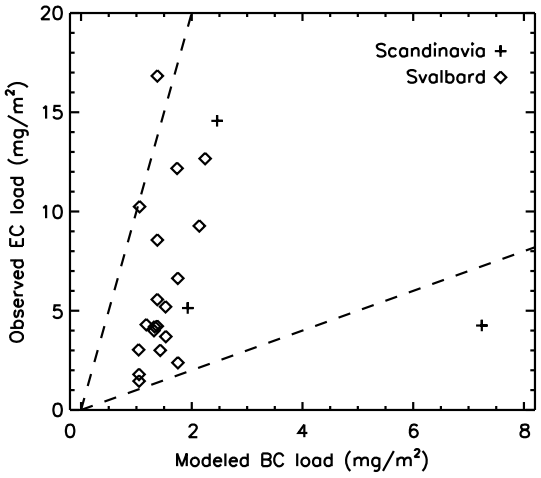

Figure 5. Scatterplot of modeled BC column load and observed EC column load, in **mg/m^2**, for the column samples in Table 3. Linnébreen C6 and C7 are excluded due to local pollution. The 1:1 and 10:1 (observed:modeled) lines are indicated with dashed lines.

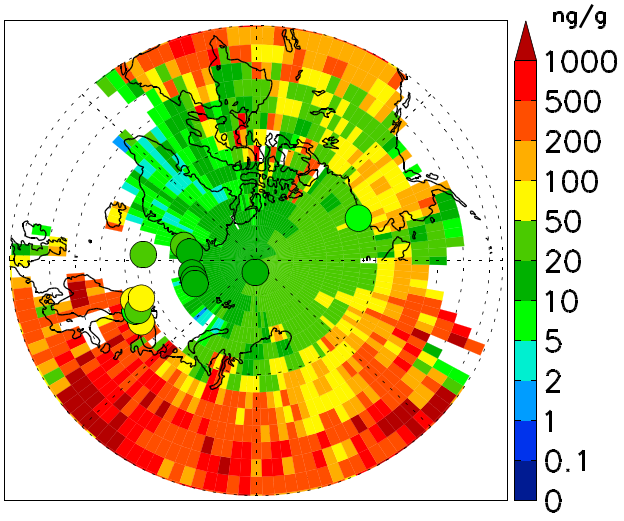

Figure 6. Mean modeled concentration of BC in surface snow (uppermost 5 cm) for March, April, and May in 2008. The medians of the surface samples done in the spring period from Table 1 are shown in colored circles. The observations from 2007 are shifted 5° to the west and observations from 2009 shifted 5° to the east for better visualization. Locally polluted Linnébreen samples are excluded from the values shown for Svalbard.

Svalbard and Scandinavia. In spring, the model overestimates the concentration at a few Scandinavian sites, but generally the model underestimates the Scandinavian surface concentrations by a factor of 1.6. In Svalbard the model underpredicts the surface concentrations in spring by a factor of 2.6. No meltwater scavenging is included in the model, and it is assumed that BC in melting snow layers remains at the surface of the snowpack during melting. Thus, the BC content in the snow column is conserved until the whole snow column has melted [*Skeie et al.*, 2011]. This will result in a positive bias in the springtime model results.

4. Discussion

4.1. EC Distribution in Snow

[28] Due to reduced emissions in North America [*Murphy et al.*, 2011] and Europe [*Legrand et al.*, 2007], recent data from Arctic atmospheric monitoring stations show a decrease in atmospheric concentrations of BC [*Eleftheriadis et al.*, 2009; *Hirdman et al.*, 2010]. *Clarke and Noone* [1985] measured BC concentrations in Arctic snow in the early 1980s and found higher levels than the median concentrations we found at the Arctic sites of Svalbard, Fram Strait, and Barrow. Their samples from near Abisko contained similar or somewhat lower concentrations than those we found there (median of their eight samples was 31 ng/g, compared to our annual medians of 32 and 51 ng/g); however, they sampled only fresh snow, which may have caused a negative bias. There are, however, methodological differences between these two data sets, and the large temporal variability in surface snow [EC] (Figure 4) shows how important the timing of sampling can be.

[29] Snow [EC] was found to increase toward late spring at the sites where concentrations were monitored throughout the snow season. The springtime increase in surface snow [EC] could be due to a springtime peak in atmospheric transport of pollutants to the Arctic [e.g., *Stohl*, 2006; *Quinn et al.*, 2007], which causes enhanced deposition, to the climatological precipitation minimum in spring which leaves the same snow surface exposed to dry deposition for a longer time, or to melting of the surface snow that leaves insoluble impurities at the surface [*Meyer and Wania*, 2008; *Doherty et al.*, 2013].

[30] The observation that most of the high surface snow [EC] events occur just after the beginning of snowmelt (Figure 4), rather than developing gradually over the course of the spring, strongly suggests that particles being left at the surface during melt are the primary driver of our observed springtime [EC] maxima. Most large [EC] spikes seen in Figure 4 are clearly associated with snow depth decreases; the one clear exception is the March 2008 spike in Abisko. The increase on Brøggerhalvøya occurred in early May, at about the same time as the first observations of temperatures above freezing in Ny-Ålesund. The other proposed factors may play a lesser role in enhancing springtime [EC] but seem not to dominate. Atmospheric BC concentrations at Zeppelin and Pallas stations have been observed to peak around March [*Eleftheriadis et al.*, 2009; *Forsström et al.*, 2009; *Hyvärinen et al.*, 2011], 1–2 months before the observed peak in snow [EC]. The climatologies for all of the sites shown in Figure 4 show minimum precipitation in spring, and the years in question were unexceptional. However, dry deposition on a stable snow pack would likely lead to a slow increase in [EC] with infrequent, episodic decreases when there was new snow, a pattern that does not dominate in Figure 4. More frequent sampling and better quantification of precipitation and surface melt would be needed to fully describe

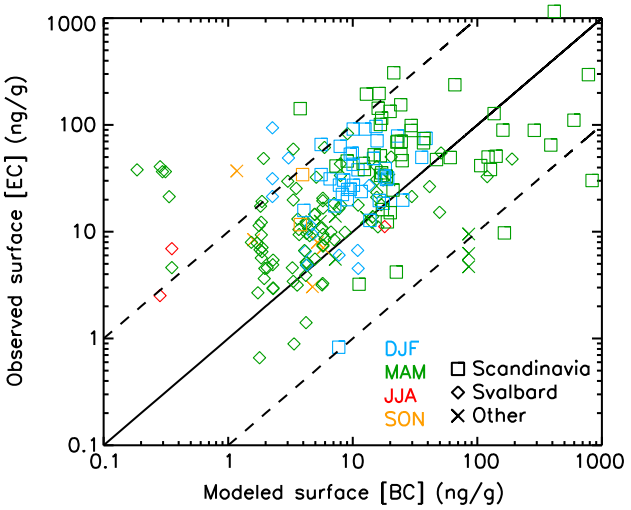

Figure 7. Observed surface snow EC concentrations against modeled BC concentrations. Winter (DJF, December-January-February) observations are in blue, spring (MAM, March-April-May) observations in green, summer (JJA, June-July-August) observations in red, and autumn (SON, September-October-November) observations in orange. The solid line shows a one-to-one correspondence and the dashed lines a factor of 10 difference between the model results and the observations.

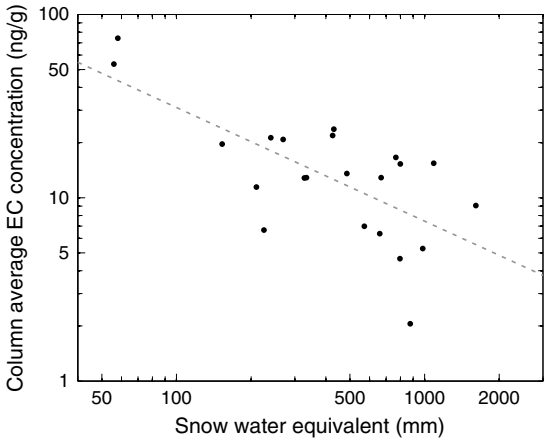

Figure 8. Column-average EC concentration over the depth of the seasonal snow pack (column load divided by mass of snow per unit area) versus the snow water equivalent in the seasonal snow pack. The dashed line shows a least squares linear regression to the logarithm of the data.

the roles that dry and wet deposition and snowmelt play in creating the seasonal variations in [EC] in surface snow.

[31] For a given concentration of BC in the atmosphere, one would expect lower concentrations, on average, in the snow pack at locations with more precipitation. This effect of greater precipitation amount diluting the BC in the snow should be especially strong if dry deposition dominates, though it would likely also appear even if wet deposition dominates. Figure 8 shows the column-average [EC] versus snow water equivalent, based on data from Table 3, excluding the locally polluted Linnébreen samples (column-average [EC] is the column load of EC divided by the mass of snow per unit area). As most of these sites experience limited wintertime snowmelt, snow water equivalent is a reasonable proxy for seasonal snowfall. On glaciers, the column was defined as the snow surface to the previous summer layer. The data in Figure 8 suggest that a negative correlation is apparent in our column samples, though accurately quantifying the relationship would require more systematic sampling in specific regions with spatially varying precipitation but spatially uniform atmospheric BC concentrations.

4.2. Oslo CTM2 Model Comparison

[32] The model generally shows lower BC concentrations in snow than those observed, with column loads up to a factor of 10 lower than observed. *Skeie et al*. [2011] showed that the model underestimates BC in the atmosphere and snow during spring (the period in which most of the observations were conducted), compared with surface measurements and flight campaigns. The Oslo CTM2 model was included in the multimodel study by *Lee et al*. [2013], which showed that the Oslo CTM2, like other models, fails to reproduce the seasonality in the Arctic atmospheric BC concentration, with a significant underestimation in winter and spring. Since atmospheric concentrations in winter and spring are underestimated in the Arctic, the deposition will also be too low. This error will be most readily seen in the modeled column load of BC in snow, which is the accumulated BC over the whole snow season.

[33] There are several reasons for the underestimation of atmospheric BC concentration in the Arctic. As *Skeie et al*. [2011] point out, the model forcing might be missing emissions of biomass burning in midlatitudes to high latitudes during spring. There is also no seasonal variation in the fossil fuel and biofuel emissions used in the model simulations. *Stohl et al*. [2013] showed that including seasonal variation in domestic emissions, as well as improved emissions from gas flaring in northern Russia, enhanced the winter and spring BC concentration in the Arctic. In the modeling, there are also uncertainties related to the aging processes of black carbon, its atmospheric transport, and the removal processes of BC from the atmosphere [*Skeie et al*., 2011]. Wet removal is a major source of uncertainty in modeling of atmospheric BC [e.g. *Shindell et al*., 2008; *Koch et al*., 2009; *Vignati et al*., 2010; *Schwarz et al*., 2010], and several studies have pointed to wet removal as the key uncertainty in the modeling of the seasonal cycle of Arctic BC concentration [*Wang et al*., 2013b; *Lee et al*., 2013; *Browse et al*., 2012; *Garret et al*., 2010].

[34] We have compared the modeled snow column loads of BC (Figure 5) and the modeled surface snow BC concentrations (Figures 6 and 7) in coarse grid boxes of $2.8 \times 2.8°$ with point measurements of [EC]. We expect significant variability within such a large grid box, and the point measurements may be made at locations that differ from the mean conditions for the region. The model-predicted snow-free conditions for many of the study sites that had shallow observed snowpacks (less than about 0.5 m) and the modeled seasonal snow depths were generally lower than the column samples. This may indicate a sampling bias or a precipitation bias in the model; in either case, having too little snow in the model compared to the column sample will give a modeled column load that is too small, even if the modeled concentrations are correct.

4.3. Variability in Snow

[35] Column loads of BC are less affected than near-surface concentrations by transient processes acting on a layer of snow, and they provide an integrated seasonal signal of accumulation and deposition. As a result they should show less small-scale spatial variability. The data in Table 3, excluding Linnébreen, show a positive correlation (coefficient 0.64) between h_{SWE}, a proxy for precipitation, and column loads of EC. A similar correlation (coefficient 0.53) is found when considering only the Svalbard data. Assuming that dry deposition rates do not vary much across Svalbard, this positive correlation suggests that wet deposition is an important mechanism for depositing BC in Arctic snow. More samples in different precipitation and pollution regimes are needed to further quantify this observation.

[36] While column loads are useful for examining integrated signals, it is the BC concentration in near-surface snow that has the strongest impact on the absorption of solar radiation, and here we found large meter-scale variability in [EC] that cannot be explained by methodological uncertainties (section 4.1). Spatial variability in snow properties at different scales has been presented by earlier studies [*Stenberg et al*., 1999; *Gusain et al*., 2006; *Karlöf et al*., 2006; *Svensson et al*., 2013]. Wind-driven drifting causes relocation, densification, and ridging of snow, enhancing the spatial variability of BC concentrations in snow [*Svensson et al*., 2013]. Also, greater horizontal variability is

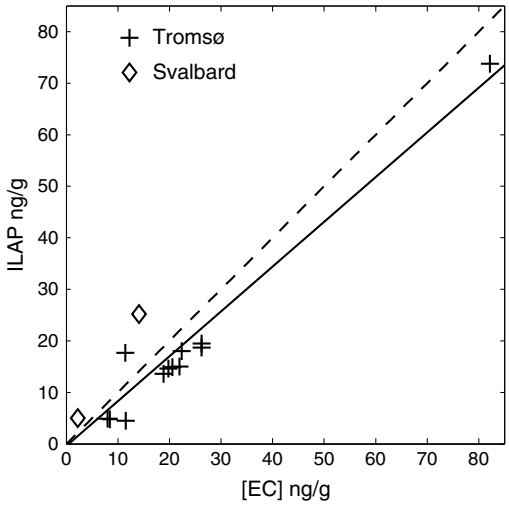

Figure 9. Intercomparison of measurements from the same samples of concentrations of insoluble light-absorbing particles (ILAP) from the ISSW method and of concentrations of EC from the thermal optical method used in the present study. The dashed line indicates the 1-to-1 line, while the solid line shows a linear fit to the data (ILAP = 0.869[EC] − 0.364).

observed in samples from areas with large vertical gradients in impurity concentrations [*Doherty et al*., 2010]. According to *Aamaas et al*. [2011], postdepositional processes alter BC concentrations in the snow pack and tend to increase the concentrations through sublimation.

[37] The side-by-side ratios of the replicate samples in this study (Figure 2) show a slightly larger spread than those reported by *Doherty et al*. [2010], whose results from samples collected less than 1 m apart were typically within 20–30% of each other. They observed the largest variability in samples collected closest to sources, which is supported by our observation that variability increases with concentration.

[38] *Aamaas et al*. [2011] measured vertical profiles of [EC] in snow using analytical methods identical to this study but performing vertical sampling based on observed stratigraphic layers rather than from constant depths. Their measurements include four snow pits, each 1 m from the previous, which show relatively low variability, with [EC] medians within 18% of each other. This low variability within stratigraphic layers suggests that the spatial variability seen in our data may be due, in part, to variations in which layers were nearest the surface at each sampling location.

[39] In a study from northern Scandinavia, *Svensson* [2011] found four times higher horizontal variability in [EC] in snow at a wind-exposed site compared to snow at a wind-protected site. *Svensson*'s sampling design included a grid of 25 pits, 5 m apart, at two sites and reported median values within 22% of each other at the wind-protected site and within 81% of each other at the wind-exposed site. We find no such strong covariance between the spatial variability and the degree to which the site is exposed to wind.

[40] Some of our sites, such as the town of Tromsø, have local BC sources. We have indicated these sites in Tables 1–3. *Vestreng et al*. [2009] estimated that annual BC emissions in Svalbard total 61 t, mainly from the coal plants in the settlements of Longyearbyen and Barentsburg. The study by *Aamaas et al*. [2011] supports the assumption that none of the Svalbard sites in our study suffers from pollution from local settlements, except Linnébreen (samples A4–5 and C6–7). The relatively high values measured in Inglefieldbukta (samples A19–21) suggest local pollution. The closest settlement, Sveagruva, is a coal mining settlement with considerable emissions [*Aamaas et al*., 2011], located about 40 km west of the sampling site. However, because of prevailing easterly winds, the snow in Inglefieldbukta is not expected to be influenced by the settlement.

4.4. Method Uncertainties

[41] The EC concentrations presented in this study are likely underestimates of real [EC]. EC particles may become stuck to the sampling jar or plastic bag or to the funnel during filtration. There will also be some undercatch due to particles that are not trapped on the quartz filter. Additional analytical uncertainties include any sampling uncertainty related to uneven filter loading and the imperfect ability of the thermal optical method to differentiate EC from carbonate and organic carbon. As discussed in section 4.1, based on *Svensson*'s [2011] study of the variability in EC mass derived from repeated analysis with the thermal optical method from individual filters, the variability due to uneven filter loading and method uncertainties accounts for less than 20% of the total variability of [EC] observed at a site (equation (1)). The remaining variability in the replicate data is primarily attributed to natural variability in snow, though variable loss of EC to the sampling container and funnel could also contribute.

[42] The undercatch of the quartz filters was studied with six samples which were mixed carefully and divided into two parts each. The first part was passed through a Nuclepore 0.4 μm filter, and the second part was first passed through a quartz filter then through a 0.4 μm Nuclepore filter. The Nuclepore filters were analyzed with the ISSW method at the University of Washington. Comparing the BC derived from the six pairs of Nuclepore filters indicates an average undercatch on the quartz filters of 22%. For the two samples from remote sites in Svalbard, the undercatch was 30%, and for four samples collected close to the town of Tromsø, it was 18%. These results have been corrected for the estimated undercatch of Nuclepore filters [*Doherty et al*., 2010]. We do not have enough undercatch samples to confidently develop a quantitative correction, so the undercatch values reported here provide an estimate for the related error in our data. Any variability in the undercatch would also contribute to the variability we report from the replicate samples.

[43] Some studies have tried to estimate the loss of particles to containers. Once the sample is in liquid form, hydrophobic soot might be left behind in the glass jar or the funnel [*Ogren and Charlson*, 1983; *Clarke and Noone*, 1985]. *Ming et al*. [2008] found the loss of particles in a similar filtering process to be less than 5%. For the samples collected in plastic bags, particles can attach to surfactant from the plastic, which then remains in the sampling jar [*Hegg et al*., 2010; *Doherty et al*., 2013; *Wang et al*., 2013a]. *Wang et al*. [2013a] introduced a correction factor dependent on BC concentration, which is at its maximum (about 1.5) for smallest concentrations.

[44] Figure 9 shows an intercomparison between the ISSW method used by [*Doherty et al*., 2010] and the thermal optical method of this study. Fourteen samples were well mixed after melting and divided for filtration using the two methods. [EC] measured by the thermal optical and ILAP (insoluble light-absorbing particulates) concentrations measured by ISSW were well correlated and of comparable magnitude, with ILAP concentrations averaging 85% of [EC]. The ISSW method overestimates BC for samples containing mineral dust [*Schwarz et al*., 2012], and the quartz filter used in the thermal optical method has greater undercatch, especially of aerosol transported over long distances. This combination of different error sources seems to make the comparison sensitive to the pollution regime: the two samples collected in remote but mineral-dust-rich Svalbard resulted in [EC] that averaged half the ILAP concentrations, while samples collected downtown or close to Tromsø resulted in [EC] that averaged 1.3 times the ILAP concentration. The two methods are based on different physical principles, with no perfect agreement expected, but the conversion from the thermal optical method using the NIOSH-5040 protocol to EUSAAR2 has improved the agreement between the two methods substantially. Using NIOSH-5040, a factor of 2 difference to the ISSW method was commonly seen [*Doherty et al*., 2010].

[45] BC concentrations measured in snow in 2007 by *Doherty et al*. [2010] on Brøggerhalvøya (7–16 ng/g, ISSW method) compare well with those in this study (median 8.3 ng/g, thermal optical). Their measurements in Tromsø in 2008 (~19 ng/g) were lower than the median of 51 ng/g in this study, which can be explained by the fact that their sampling site was on a mountain plateau above town, while ours were mostly from downtown. Samples collected during a joint field campaign in spring 2008 in Barrow are in good agreement.

5. Conclusion

[46] A large number of snow samples were collected in Scandinavia, Svalbard, Alaska, and on Arctic sea ice, both from surface snow and from vertical profiles through the snow column. The samples were analyzed for elemental carbon (EC) concentration using a thermal optical method.

[47] Systematically higher values of snow EC concentration were observed in Scandinavia than in the Arctic sites, a feature that is also seen in the chemical transport model Oslo CTM2. The Oslo CTM2 typically underestimates snow black carbon concentrations (both surface concentrations and overall column loads). As the measured EC levels in snow are likely underestimated, the gap between real and modeled concentrations is likely higher than presented in this study.

[48] A rapid increase in EC concentrations in surface snow, of up to an order of magnitude, was observed at monitoring sites at the onset of snowmelt in April or May, 1–2 months after the annual peak in atmospheric concentrations. These increases typically coincide with the onset of rapid snowmelt and likely result from insoluble particles being left at the surface as meltwater runs off.

[49] Meter-scale variability in EC concentrations in snow was found to increase with concentration. The standard deviation of multiple samples from a given site was about 37% of the mean concentration and seems to be driven by real variability in the snow pack, rather than only methodological uncertainties. This variability needs to be taken into consideration when planning future sampling routines and when interpreting existing results.

[50] The comparison between the thermal optical method and ISSW, another common method for estimating black carbon in snow, has improved substantially since the EUSAAR2 temperature came into use in place of the older NIOSH-5040 sequence. After the conversion the two methods are in good agreement, but more intercomparison samples are needed to determine whether their covariance depends on the type of aerosol.

[51] **Acknowledgments.** We express our gratitude to the following persons who helped in collecting the samples: G. Rotchky, M. Nicolaus, A. Nicolaus, O-M. Olsen, J. Kohler, M. Björkman, O-P. Mattila, E. Beaudon, T. Martma, C. Vega, B. Møller, F. Pinczon du Sel, and E. Brossier. We thank the personnel at the Sverdrup, Abisko, Pallas, and Tarfala stations and on Tara for helping us to collect samples; personnel at ITM, Stockholm University for filter analysis; and the meteorological office at Tromsø for allowing us to use their measurement field for sampling. J-C. Gallet and D. Divine provided helpful discussions. S. Warren and S. Doherty shared their expertise and worked with us on the ISSW intercomparison and the undercatch study. Snow depth data for Abisko were provided by Abisko Scientific Research Station and the Swedish Polar Research Secretariat and in Pallas by the Finnish Meteorological Institute. J. Kohler provided some of the snow density measurements from Svalbard. The Norwegian Polar Institute's (NPI) Mapping Section provided the cartography used in the figures. Funding for this work was provided by the Research Council of Norway (Norklima and PolRes programs) through the projects "Climate effects of reducing black carbon emissions" (165064), "Measurements of BC in Arctic snow" (178912), VAUUAV (184724), and "Svalbard ice cores and climate variability" (178764), in addition to NPI internal funding. This publication is a contribution to Cryosphere-Atmosphere Interactions in a Changing Arctic Climate (CRAICC) a Top-level Research Initiative (TRI). Additional support was provided by Formas-The Swedish Research Council for Environment through the project "Black and White," and through the projects ECLIPSE, funded by the European Union, and SLAC, funded by the Research Council of Norway.

References

Aamaas, B., C. E. Bøggild, F. Stordal, T. Berntsen, K. Holmén, and J. Ström (2011), Elemental carbon deposition to Svalbard snow from Norwegian settlements and long-range transport, *Tellus B*, *63*(3), 340–351, doi:10.1111/j.1600-0889.2011.00531.x.

Andreae, M. O., and A. Gelencsér (2006), Black carbon or brown carbon? The nature of light-absorbing carbonaceous aerosols, *Atmos. Chem. Phys.*, *6*, 3131–3148, doi:10.5194/acp-6-3131-2006.

Berntsen, T., J. Fuglestvedt, G. Myhre, F. Stordal, and T. F. Berglen (2006), Abatement of greenhouse gases: Does location matter?, *Clim. Change*, *74*(4), 377–411, doi:10.1007/s10584-006-0433-4.

Birch, M. E. (2003), Diesel particulate matter (as elemental carbon): Method 5040, *NIOSH Man. Occup. Saf. Health*, *3*, 1–5.

Birch, M. E., and R. A. Cary (1996), Elemental carbon-based method for monitoring occupational exposures to particulate diesel exhaust, *Aerosol Sci. Technol.*, *25*(3), 221–241, doi:10.1080/02786829608965393.

Bond, T. C., D. G. Streets, K. F. Yarber, S. M. Nelson, J.-H. Woo, and Z. Klimont (2004), A technology-based global inventory of black and organic carbon emissions from combustion, *J. Geophys. Res.*, *109* D14203, doi:10.1029/2003JD003697.

Bond, T. C., et al. (2013), Bounding the role of black carbon in the climate system: A scientific assessment, *J. Geophys. Res. Atmos.*, *118*, 5380–5552, doi:10.1002/jgrd.50171.

Browse, J., K. S. Carslaw, S. R. Arnold, K. Pringle, and O. Boucher (2012), The scavenging processes controlling the seasonal cycle in Arctic sulphate and black carbon aerosol, *Atmos. Chem. Phys.*, *12*, 6775–6798.

Cavalli, F., M. Viana, K. E. Yttri, J. Genberg, and J.-P. Putaud (2010), Toward a standardised thermal-optical protocol for measuring atmospheric organic and elemental carbon: The EUSAAR protocol, *Atmos. Meas. Tech.*, *3*(1), 79–89, doi:10.5194/amt-3-79-2010.

Clarke, A., and K. Noone (1985), Soot in the arctic snowpack: A cause for perturbations in radiative transfer, *Atmos. Environ.*, *19*(12), 2045–2053, doi:10.1016/j.atmosenv.2007.10.059.

Doherty, S. J., S. G. Warren, T. C. Grenfell, A. D. Clarke, and R. E. Brandt (2010), Light-absorbing impurities in Arctic snow, *Atmos. Chem. Phys.*, *10*(23), 11,647–11,680, doi:10.5194/acp-10-11647-2010.

Doherty, S. J., T. C. Grenfell, S. Forsström, D. L. Hegg, R. E. Brandt, and S. G. Warren (2013), Observed vertical redistribution of black carbon and other insoluble light-absorbing particles in melting snow, *J. Geophys. Res. Atmos.*, *118*, 5553–5569, doi:10.1002/jgrd.50235.

Eleftheriadis, K., S. Vratolis, and S. Nyeki (2009), Aerosol black carbon in the European Arctic: Measurements at Zeppelin station, Ny-Ålesund, Svalbard from 1998–2007, *Geophys. Res. Lett.*, *36* L02809, doi:10.1029/2008GL035741.

Flanner, M. G., C. S. Zender, J. T. Randerson, and P. J. Rasch (2007), Present-day climate forcing and response from black carbon in snow, *J. Geophys. Res.*, *112* D11202, doi:10.1029/2006JD008003.

Forsström, S., J. Ström, C. A. Pedersen, E. Isaksson, and S. Gerland (2009), Elemental carbon distribution in Svalbard snow, *J. Geophys. Res.*, *114*, D19112, doi:10.1029/2008JD011480.

Forsström, S., S. Gerland, and C. A. Pedersen (2011), Thickness and density of snow-covered sea ice and hydrostatic equilibrium assumption from in situ measurements in Fram Strait, the Barents Sea and the Svalbard coast, *Ann. Glaciol.*, *52*(57), 261–270, doi:10.3189/172756411795931598.

Grenfell, T. C., B. Light, and M. Sturm (2002), Spatial distribution and radiative effects of soot in the snow and sea ice during the SHEBA experiment, *J. Geophys. Res.*, *107*(C108032), doi:10.1029/2000JC000414.

Gusain, H. S., C. Chandel, and A. Ganju (2006), Spatial variation of snow-cover properties on small uniform mountain slopes in the Greater Himalayan region, *Curr. Sci.*, *91*(5), 672–677.

Hegg, D. A., S. G. Warren, T. C. Grenfell, S. J. Doherty, T. V. Larson, and A. D. Clarke (2009), Source attribution of black carbon in Arctic snow, *Environ. Sci. Technol.*, *43*, 4016–4021.

Hegg, D. A., S. G. Warren, T. C. Grenfell, S. J. Doherty, and A. D. Clarke (2010), Sources of light-absorbing aerosol in arctic snow and their seasonal variation, *Atmos. Chem. Phys. Discuss.*, *10*(6), 13,755–13,796, doi:10.5194/acpd-10-13755-2010.

Hirdman, D., J. F. Burkhart, H. Sodemann, S. Eckhardt, A. Jefferson, P. K. Quinn, S. Sharma, J. Ström, and A. Stohl (2010), Long-term trends of black carbon and sulphate aerosol in the Arctic: Changes in atmospheric transport and source region emissions, *Atmos. Chem. Phys.*, *10*(19), 9351–9368, doi:10.5194/acp-10-9351-2010.

Huang, J., Q. Fu, W. Zhang, X. Wang, R. Zhang, H. Ye, and S. G. Warren (2010), Dust and black carbon in seasonal snow across northern China, *Bull. Am. Meteorol. Soc.*, *92*, 175–181.

Hyvärinen, A.-P., et al. (2011), Aerosol black carbon at five background measurement sites over Finland, a gateway to the Arctic, *Atmos. Environ.*, *45*(24), 4042–4050, doi:10.1016/j.atmosenv.2011.04.026.

Karlöf, L., D. P. Winebrenner, and D. B. Percival (2006), How representative is a time series derived from a firn core? A study at a low-accumulation site on the Antarctic plateau, *J. Geophys. Res.*, *111*, F04001, doi:10.1029/2006JF000552.

Kaspari, S. D., M. Schwikowski, M. Gysel, M. G. Flanner, S. Kang, S. Hou, and P. A. Mayewski (2011), Recent increase in black carbon concentrations from a Mt. Everest ice core spanning 1860–2000 AD, *Geophys. Res. Lett.*, *38*, L04703, doi:10.1029/2010GL046096.

Koch, D., et al. (2009), Evaluation of black carbon estimations in global aerosol models, *Atmos. Chem. Phys.*, (November), *9*, 9001–9026.

Lee, Y. H., et al. (2013), Evaluation of preindustrial to present-day black carbon and its albedo forcing from Atmospheric Chemistry and Climate Model Intercomparison Project (ACCMIP), *Atmos. Chem. Phys.*, *13*(5), 2607–2634.

Legrand, M., S. Preunkert, M. Schock, M. Cerqueira, A. Kasper-Giebl, J. Afonso, C. Pio, A. Gelencsér, and I. Dombrowski-Etchevers (2007), Major 20th century changes of carbonaceous aerosol components (EC, WinOC, DOC, HULIS, carboxylic acids, and cellulose) derived from Alpine ice cores, *J. Geophys. Res.*, *112*, D23S11, doi:10.1029/2006JD008080.

McConnell, J. R., R. Edwards, G. L. Kok, M. G. Flanner, C. S. Zender, E. S. Saltzman, J. R. Banta, D. R. Pasteris, M. M. Carter, and J. D. W. Kahl (2007), 20th-century industrial black carbon emissions altered Arctic climate forcing, *Science*, *317*(5843), 1381–4, doi:10.1126/science.1144856.

Meyer, T., and F. Wania (2008), Organic contaminant amplification during snowmelt, *Water Res.*, *42*(8–9), 1847–65, doi:10.1016/j.watres.2007.12.016.

Ming, J., H. Cachier, C. Xiao, D. Qin, S. Kang, S. Hou, and J. Xu (2008), Black carbon record based on a shallow Himalayan ice core and its climatic implications, *Atmos. Chem. Phys.*, *8*(5), 1343–1352, doi:10.5194/acp-8-1343-2008.

Murphy, D. M., J. C. Chow, E. M. Leibensperger, W. C. Malm, M. Pitchford, B. A. Schichtel, J. G. Watson, and W. H. White (2011), Decreases in elemental carbon and fine particle mass in the United States, *Atmos. Chem. Phys.*, *11*(10), 4679–4686, doi:10.5194/acp-11-4679-2011.

Myhre, G., et al. (2009), Modelled radiative forcing of the direct aerosol effect with multi-observation evaluation, *Atmos. Chem. Phys.*, *9*, 1365–1392, doi:10.5194/acp-9-1365-2009.

Ogren, J. A., and R. Charlson (1983), Elemental carbon in the atmosphere: Cycle and lifetime, *Tellus B*, *35*, 241–245, doi:10.1111/j.1600-0889.1983.tb00027.x.

Petzold, A., et al. (2013), Recommendations for reporting "black carbon" measurements, *Atmos. Chem. Phys.*, *13*, 8365–8379, doi:10.5194/acp-13-8365-2013.

Quinn, P. K., G. Shaw, E. Andrews, E. G. Dutton, T. Ruoho-Airola, and S. L. Gong (2007), Arctic haze: Current trends and knowledge gaps, *Tellus B*, *59*(1), 99–114, doi:10.1111/j.1600-0889.2006.00238.x.

Rasmus, S. (2005), Snow pack structure characteristics in Finland—Measurements and modelling (PhD thesis), University of Helsinki.

Riahi, K., S. Rao, V. Krey, C. Cho, V. Chirkov, G. Fischer, G. Kindermann, N. Nakicenovic, and P. Rafaj (2011), RCP 8.5—A scenario of comparatively high greenhouse gas emissions, *Clim. Change*, *109*(1–2), 33–57, doi:10.1007/s10584-011-0149-y.

Rypdal, K., N. Rive, T. K. Berntsen, Z. Klimont, T. K. Mideksa, G. Myhre, and R. B. Skeie (2009), Costs and global impacts of black carbon abatement strategies, *Tellus B*, *61*(4), 625–641, doi:10.1111/j.1600-0889.2009.00430.x.

Schwarz, J. P., et al. (2008), Measurement of the mixing state, mass, and optical size of individual black carbon particles in urban and biomass burning emissions, *Geophys. Res. Lett.*, *35*, L13810, doi:10.1029/2008GL033968.

Schwarz, J. P., J. R. Spackman, R. S. Gao, L. A. Watts, P. Stier, M. Schulz, S. M. Davis, S. C. Wofsy, and D. W. Fahey (2010), Global-scale black carbon profiles observed in the remote atmosphere and compared to models, *Geophys. Res. Lett.*, *37*, L18812, doi:10.1029/2010GL044372.

Schwarz, J. P., S. J. Doherty, F. Li, S. T. Ruggiero, C. E. Tanner, A. E. Perring, R. S. Gao, and D. W. Fahey (2012), Assessing single particle soot photometer and integrating sphere/integrating sandwich spectrophotometer measurement techniques for quantifying black carbon concentration in snow, *Atmos. Meas. Tech.*, *5*(11), 2581–2592, doi:10.5194/amt-5-2581-2012.

Shindell, D. T., et al. (2008), A multi-model assessment of pollution transport to the Arctic, *Atmos. Chem. Phys.*, *8*, 5353–5372, doi:10.5194/acp-8-5353-2008.

Skeie, R. B., T. Berntsen, G. Myhre, C. A. Pedersen, J. Ström, S. Gerland, and J. A. Ogren (2011), Black carbon in the atmosphere and snow, from pre-industrial times until present, *Atmos. Chem. Phys.*, *11*(14), 6809–6836, doi:10.5194/acp-11-6809-2011.

Stenberg, M., M. Hansson, P. Holmlund, and L. Karlöf (1999), Variability in snow layering and snow chemistry in the vicinity of two drill sites in western Dronning Maud Land, Antarctica, *Ann. Glaciol.*, *29*(1), 33–37.

Stohl, A. (2006), Characteristics of atmospheric transport into the Arctic troposphere, *J. Geophys. Res.*, *111*, D11306, doi:10.1029/2005JD006888.

Stohl, A., Z. Klimont, S. Eckhardt, K. Kupiainen, V. P. Shevchenko, V. M. Kopeikin, and A. N. Novigatsky (2013), Black carbon in the Arctic: The underestimated role of gas flaring and residential combustion emissions, *Atmos. Chem. Phys.*, *13*, 8833–8855, doi:10.5194/acp-13-8833-2013.

Svensson, J. (2011), Horizontal meter scale variability of elemental carbon in surface snow (masters thesis), Stockholm University.

Svensson, J., J. Ström, M. Hansson, H. Lihavainen, and V.-M. Kerminen (2013), Observed metre scale horizontal variability of elemental carbon in surface snow, *Environ. Res. Lett.*, *8*, 034012, doi:10.1088/1748-9326/8/3/034012.

Van der Werf, G. R., J. T. Randerson, L. Giglio, G. J. Collatz, M. Mu, P. S. Kasibhatla, D. C. Morton, R. S. DeFries, Y. Jin, and T. T. van Leeuwen (2010), Global fire emissions and the contribution of deforestation, savanna, forest, agricultural, and peat fires (1997–2009), *Atmos. Chem. Phys.*, *10*(23), 11,707–11,735, doi:10.5194/acp-10-11707-2010.

Vestreng, V., R. Kallenborn, and E. Økstad (2009), Norwegian Arctic climate—Climate influencing emissions, scenarios and mitigation options at Svalbard.

Vignati, E., M. Karl, M. Krol, J. Wilson, P. Stier, and F. Cavalli (2010), Sources of uncertainties in modelling black carbon at the global scale, *Atmos. Chem. Phys.*, *10*, 2595–2611, doi:10.5194/acp-10-2595-2010.

Wang, X., S. J. Doherty, and J. Huang (2013a), Black carbon and other light-absorbing impurities in snow across northern China, *J. Geophys. Res. Atmos.*, *118*, 1471–1492, doi:10.1029/2012JD018291.

Wang, H., R. C. Easter, P. J. Rasch, M. Wang, X. Liu, S. J. Ghan, Y. Qian, J.-H. Yoon, P.-L. Ma, and V. Vinoj (2013b), Sensitivity of remote aerosol distributions to representation of cloud-aerosol interactions in a global climate model, *Geosci. Model Dev.*, *6*, 765–782, doi:10.5194/gmd-6-765-2013.

Warren, S. G., and A. D. Clarke (1990), Soot in the atmosphere and snow surface of Antarctica, *J. Geophys. Res.*, *95*(D2), 1811–1816, doi:10.1029/JD095iD02p01811.

Warren, S. G., R. E. Brandt, and T. C. Grenfell (2006), Visible and near-ultraviolet absorption spectrum of ice from transmission of solar radiation into snow, *Appl. Opt.*, *45*(21), 5320–34, doi:10.1364/AO.45.005320.

Watson, J. G., J. C. Chow, and L. A. Chen (2005), Summary of organic and elemental carbon / black carbon analysis methods and intercomparisons, *Aerosol Air Qual. Res.*, *5*(1), 65–102.

Ye, H., R. Zhang, J. Shi, J. Huang, S. G. Warren, and Q. Fu (2012), Black carbon in seasonal snow across northern Xinjiang in northwestern China, *Environ. Res. Lett.*, *7*, 044002, doi:10.1088/1748-9326/7/4/044002.

Zhang, R., D. A. Hegg, J. Huang, and Q. Fu (2013), Source attribution of insoluble light-absorbing particles in seasonal snow across northern China, *Atmos. Chem. Phys.*, *13*, 6091–6099.